



Technical Sciences  
Academy of Romania  
[www.jesi.astr.ro](http://www.jesi.astr.ro)

## **Journal of Engineering Sciences and Innovation**

Volume 10, Issue 3 / 2025, pp. 261 - 274

### **C. Chemical Engineering, Materials Science and Engineering**

Received 24 April 2025

Accepted 16 September 2025

Received in revised form 28 July 2025

## **Modelling of drug injection and distribution in subcutaneous tissue**

**OANA PARVULESCU<sup>1</sup>, GHEORGHITA JINESCU<sup>1,2</sup>, TANASE DOBRE<sup>1,2\*</sup>**

<sup>1</sup>National University of Science and Technology Politehnica Bucharest, Romania

<sup>2</sup>Technical Sciences Academy of Romania

**Abstract.** From the engineering point of view, the drug solutions injection into tissue is a flow problem through the needle with discharge in a resistive medium, a problem of dispersion under pressure of the injected solution around of injected location and a drug diffusion problem in the mass of tissue. Each of the three problems are analyzed by establishing a specific mathematical model and, respectively, its simulation. There is no shortage of reports on the practice of this procedure.

**Keywords:** syringe injection, needle flow, pressure in tissue, pressure dispersion, tissue drug diffusion.

### **1. Introduction**

The administration of medication, in various diseases, by subcutaneous, intravenous, intramuscular, and even per bone injection of the medical preparation, specific to each disease, was and remains, even if it has lost its use, one of the most widespread methods of rapid application of the medical product. We find today that the injection of the medical product through the needle, even if it raises 2 big problems namely: i) contamination or needle injury [1] and ii) painful injections and needle phobia [2], is still the most used technique in such treatments. It must be shown that needle-free injection systems have an interesting perspective in solving the two problems of needle injection [3]. In this sense, even if it is not the main subject of the present presentation, we present the physical modeling of the jet injection of a colored tracer through a 1.5 mm layer of skin in a gelatin deposit, with a concentration of 90 g/l. It is important to see that in this injection technique

---

\*Correspondence address: [tghdobre@gmail.com](mailto:tghdobre@gmail.com)

it is a flow process with breaking of the continuous medium (skin and tissue) due to the extremely high speed of the microjet.

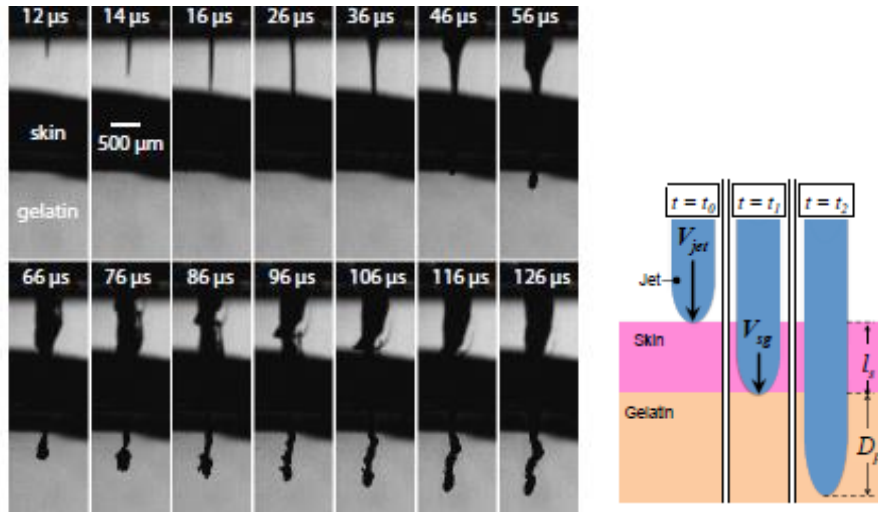


Fig. 1. Images and graphic diagram showing the dynamics of jet injection through a 1.5 mm skin supported on gelatin gel at  $V_{jet} = 160$  m/s [4].

In the case of injection of an injectable drug solution through the syringe, there are three chemical engineering interesting aspects. These are: i) the flow through the syringe needle in a resistant environment, determined by subcutaneous tissue structure; ii) the spreading (flow) of drug solution in the tissue caused by the pressure difference between the injection site and the one far from it; iii) the diffusion of active drug species from the relaxed deposit to the receptors.

## 2. Flow through the syringe needle in resistant medium

The characterization of the hydrodynamics flow through the syringe-needle system is pursued in the sense of obtaining a relationship that expresses the connection between the measured flow rate and the counter-pressure of subcutaneous tissue. A listing of the hydrodynamic variables that appear in the below relations is presented in table 1. It is worth noting here that for the injectable drug solutions it was considered that it has the physical properties of water at 30 °C. Figure 2 shows the needle-syringe piston system where the compression spring can measure the force with which the syringe piston is actuated. For usual injection conditions where  $G_v = 100$  μl/s and  $r_n = 0.08$  mm ( $G_{30}$  insulin needle) the syringe needle flow is laminar, as it is shown by the below calculation (1)

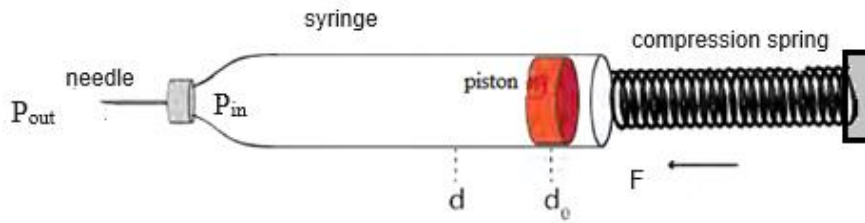


Fig. 2. Elements of the syringe-needle system characteristic of the subcutaneous injection of some drug solutions.

$$Re = \frac{2G_v}{\nu r_n} = \frac{2100 \cdot 10^{-9}}{1.24 \cdot 10^{-6} \cdot 0.081 \cdot 10^{-3}} \approx 2000 \quad (1)$$

Table 1. Characteristic elements at drug solutions flow through the syringe-needle system.

c.n	Variable name	Symbol	Unit	Usual values
1	Needle radius	$r_n$	m	$8 \cdot 10^{-5} - 4 \cdot 10^{-4}$
2	Volumetric flow rate in needele	$G_v$	$m^3/s$	$1.2 \cdot 10^{-7} - 2 \cdot 10^{-7}$
3	Velocity at beginning of boundary layer	$w_{\infty}$	m/s	0.05 – 0.25
4	Kinematic viscosity of drug solution	$\nu$	$m^2/s$	$1.24 \cdot 10^{-6}$ (la 30°C)
5	Dynamic viscosity of drug solution	$\eta$	kg/(m s)	$1.28 \cdot 10^{-3}$ (la 30°C)
6	Pressure at the needle input	$P_{in}$	Pa	$1.05 \cdot 10^5$
7	Pressure at the needle exit	$P_{out}$	Pa	$1.02 \cdot 10^5$
8	Density of drug solution	$\rho_f$	kg/m <sup>3</sup>	1000
9	Length of injection needle	$L$	m	0.0164 (insulin nd.)

This laminar flow shows that in the needle there is an important entry region where occurs the hydrodynamic boundary layer development. This boundary layer formation, as it is shown in figure 3, is responsible for additional energy consumption compared to that required for pure laminar flow through the  $r_n$  radius needle. In these conditions, in order to support a pressure loss due to the development of the boundary layer in the needle, it is proven that the entrance length of the boundary layer [5] is smaller than the length of the syringe needle. That is shown with relations (2) and (3).

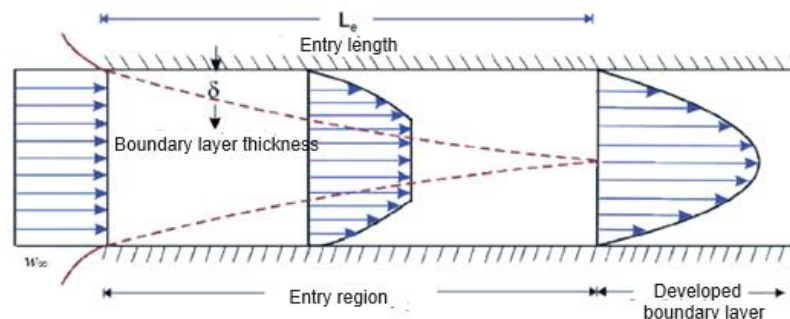


Fig. 3. Development of the boundary layer in the needle of injection syringe.

$$w_{\infty} = \frac{4G_v}{\pi r_n^2} = \frac{4100 \cdot 10^{-9}}{3.14(810^{-5})^2} = 0.2 \text{ m/s} \quad (2)$$

$$Le = 0.0456 r_n \text{ Re} = 0.0456 \cdot 810^{-5} \cdot 2000 = 6.410^{-3} = 6.4 \text{ mm} \quad (3)$$

So, the entry length value shows that the formation of the boundary layer is responsible for the consumption of additional energy compared to that required for the laminar flow through the needle of radius  $r_n$ . Under these conditions, the pressure loss when drug solution flows through the needle is expressed with the relation (4)

$$P_{in} - P_{out} = \frac{8\eta L}{\pi r_n^4} G_v + \frac{\rho_f}{\pi^2 r_n^4} G_v^2 \quad (4)$$

On the other hand, the pressure excess (overpressure) at entering of drug solution in needle is determined by the force with which the syringe piston is actuated and by the dynamic pressure corresponding to the liquid entering the needle, as it is shown by relation (5)

$$\Delta P_{in} = \frac{4F(t)}{\pi d^2} - \frac{\rho_f}{2} w_{\infty}^2 \quad (5)$$

Taking into account that at any moment this overpressure equals the difference between  $P_{in}$  and  $P_{out}$  to which is added the counterpressure from the tissue is added (6), we finally get the relationship that connects all the hydrodynamic quantities involved in the injection process (7)

$$\Delta P_{in} = P_{in} - P_{out} + CP(t) \quad (6)$$

$$\frac{4F(t,d)}{\pi d^2} - CP(t) = \frac{8\eta L}{\pi r_n^4} G_v(t) + \frac{\rho_f}{\pi^2 r_n^4} G_v^2(t) + \frac{\rho_f}{2} w_{\infty}^2 = \frac{8\eta L}{\pi r_n^4} G_v(t) \left( 1 + \frac{G_v(t)}{5.3\pi v L} \right) \quad (7)$$

Relation (7) can have three using directions, namely: i) for the known needle and syringe ( $d$  and  $r_n$  fixed) one can calibrate  $F(t,d)$  by measuring the dynamics of the flow rate  $G_v(t)$  when injecting into a non-resistive medium (injection in the air); ii) for the known syringe and unknown needle and for the dynamics of the known piston actuation force ( $F(t,d)$ ) one can find, based on the measurement of the injected flow ( $G_v(t)$ ), the conventional radius of the injection needle; iii) for the syringe and needle known by injection in air and in a resistive medium (subcutaneous medium), the dynamics of the actuation force of the piston and the counterpressure in the tissue ( $C(t)$ ) are found by measuring the flow rate of the medicinal preparation

Figure 4 shows measurements from the literature [6] for determining the back pressure in the tissue for a patient who was injected with a dose of 0.4 ml of insulin

solution, in the tissue of the belly area. For these data, an average counterpressure in the tissue of 152 mbar is obtained by calculation, as it results from values computed with relation (8) where  $G_{va}(t)$  and  $G_{vt}(t)$  are correspondent values of injection flow rate in air respectively in tissue.

$$C(t) = \frac{8\eta L}{\pi r_n^4} G_{va}(t) \left( 1 + \frac{G_{va}(t)}{5.3\pi\nu L} \right) - \frac{8\eta L}{\pi r_n^4} G_{vt}(t) \left( 1 + \frac{G_{vt}(t)}{5.3\pi\nu L} \right) \quad (8)$$

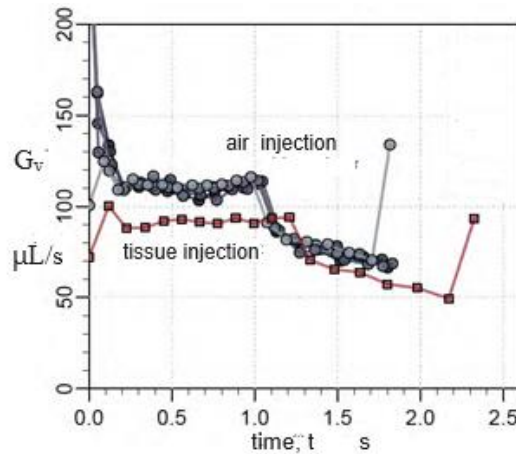


Fig. 4. Flow rate dynamics during injection of an insulin drug solution in air and in a patient tissue ( $r_n = 8 \cdot 10^{-5}$  m,  $d = 0.005$  m,  $F(t)_{\text{mean}} = 4$  N)

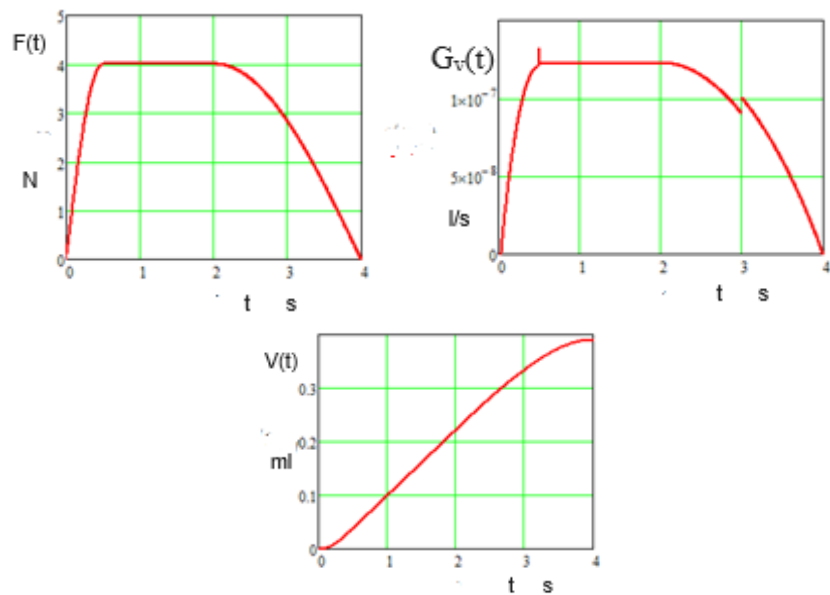


Fig. 5. Injection simulation of an insulin solution with needle-syringe system having  $r_n = 8 \cdot 10^{-5}$  m,  $L = 0.016$  m, and  $d = 0.005$  m, in a resistive medium with  $C(t) = 220$  mbar at  $t < 0.5$  s, respectively  $C(t) = 180$  mbar at  $t > 0.5$  s.

These measurements reported to other patients [6], are concentrated in table 2 with the purpose to show the variability of  $C(t)_{mean}$  upon individual patient tissue and on volume of injected dose.

Table 2. Variability by patient and operating technique of average back pressure in the tissue when injecting an insulin solution ( $r_n = 8 \cdot 10^{-5}$  m,  $d = 0.005$  m,  $F(t)_{mean} = 4$  N)

Patient	Injected dose ml	$(F(t)_{max} - F(t)_{min})/F_{medium}$	CP (t) <sub>mean</sub> mbar	$\Delta CP(t)_{mean}$ mbar
1	0.48	0.21	190	27
2	0.24	0.25	702	81
3	0.21	0.27	963	114
4	0.24	0.25	642	141
5	0.34	0.23	998	83
6	0.18	0.3	190	156

### 3. Flow of the drug solution into the tissue due to pressure from the injection site

The second analysis problem starts from the fact that during the injection and immediately after the injection in the tissue, depending on its properties, a microsphere is formed in which the pressure is practically equal to the injection counterpressure (figure 6). Since this pressure is higher than that of the adjacent medium, a flow process will take place in tissue as long as there is a pressure gradient here.

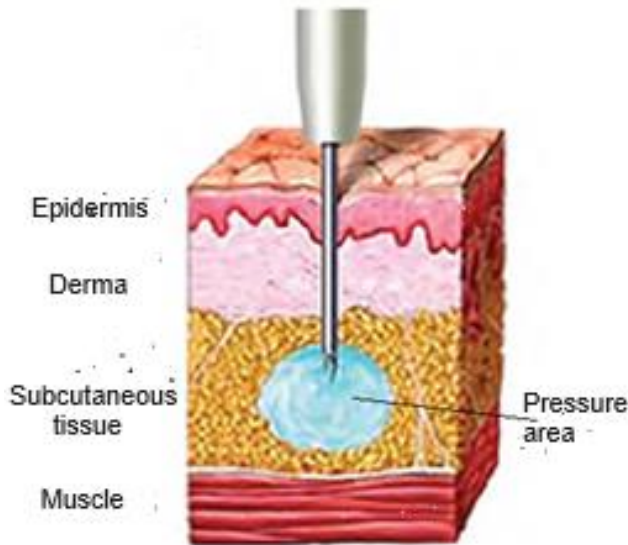


Fig. 6. End of the subcutaneous injection of a drug solution (adaptation according to [6] and [7]).

In expressing of model referring to pressure dynamics around the injection zone, it uses the process variables mentioned in table 3.

The first relationship used in establishing the pressure dynamics in injection area is expressed by the connection between the pressure gradient and the gradient of the liquid fraction in the tissue (9).

$$P(r,t) - P_0 = \alpha(\varepsilon(r,t) - \varepsilon_0). \quad (9)$$

The fact that in tissue, because of the pressure gradient induced by the injection, begin the flow of drug solution is expressed by relation (10) and (11), last relation being the continuity equation of the flow.

$$w = -\frac{\chi}{\eta} \nabla p \quad (10)$$

$$\frac{\partial \rho}{\partial t} + \nabla(\rho w) = q(r,t) \quad (11)$$

Table 3. Variables considered in expression of pressure dynamics in area of subcutaneous injection of drug solution.

c.n	Variable name	Symbol	Unit	Usual values
1	Pressure inside of stressed tissue	$P(r,t)$	Pa	CP(t) value table 2
2	Pressure inside of unstressed tissue	$P_0$	Pa	$10^5$
3	Liquid fraction in pressed tissue	$\varepsilon(r,t)$	$\text{m}^3/\text{m}^3$	$0.4 \approx 0.6$
4	Liquid fraction in unpressed tissue	$\varepsilon_0$	$\text{m}^3/\text{m}^3$	$0.5-0.7$
5	The modulus of pressure-fraction dependence of liquid inside of tissue	$\alpha$	Pa	$(0.8 - 1.4) 10^5$
6	Mean liquid velocity in tissue	$w$	m/s	0.0005
7	Injection specific flow rate in volume	$q(r,t)$	$\text{kg}/(\text{m}^2\text{s})$	0.12 -0.24
8	Drug solution density	$\rho_f$	$\text{kg}/\text{m}^3$	1000
9	Liquid viscosity in tissue	$\eta$	$\text{kg}/(\text{m s})$	$1.2 \cdot 10^{-3}$

The density of the liquid in tissue can be expressed as a function of injected solution drug and the density of current liquid from tissue, as it is shown by relation (12). Combining relations (9) - (12) we obtain the equation, with partly derivates, expressing the pressure dynamics in the injected area. This dynamic is expressed by relation (13). In concrete terms, the patients who have had a drug solution administered by subcutaneous injection, the area with pressure in the tissue feels like a slightly harder area, which gives way, and which decreases quickly over time.

$$\rho = \rho_f \frac{V_f}{V} = \rho_f \varepsilon(r,t) \quad (12)$$

$$\frac{\partial p}{\partial t} = \frac{\chi}{\mu} \nabla \left( (\alpha \varepsilon_0 + p - p_0) \nabla p \right) + \alpha \frac{q(r,t)}{\rho_f} \quad (13)$$

The source, which is the last term from relation (13), can be removed by replacing it from condition (14). That expresses the flow continuity at the tip of the needle. Here by  $q$  the product  $q(r,t)\delta(t)$  was considered, which would show an introduction (injection) type of Dirac function of drug solution in tissue. As previously shown, the flow at the tip of the needle verifies the Darcy relation (15).

$$4\pi_n^2 (\varepsilon w_r) = G_v(t) = \frac{4}{3} \pi_n^3 \int_V \frac{q}{\rho_f} dV \quad (14)$$

$$\frac{\partial p}{\partial r} \Big|_{r=r_n} = - \frac{\eta}{4\pi r_n^2 \varepsilon_0 \chi} G_v(t) \quad (15)$$

With the above considerations, relation (13) can be arranged by introducing, as is very clear, the consideration of the radial pressure distribution as well as the fact that  $p-p_0$  can be much smaller than the product  $\alpha\varepsilon_0$ . Thus, the pressure diffusion equation for injection area (16) is obtained, where the pressure diffusion coefficient is given by the relation (16) and the source term is related to average flow rate of the injected drug solution.

$$\frac{\partial p}{\partial t} = D \frac{\partial^2 p}{\partial r^2} + \frac{\rho_f G_{vmean}}{4\pi r^2} \delta(r) \quad (16)$$

$$D = \frac{\chi}{\eta} \alpha \varepsilon_0 \quad (17)$$

From the way presentation of establishment of the pressure diffusion equation in the adipose tissue (16), it can be deduced that here we have a case semi-infinite environment diffusion process. An analytical, respectively numerical, solution of the pressure distribution in the injected area can be obtained by attaching the univocity conditions to the pressure diffusion equation model (16). They express:

- the initial pressure state in the tissue at starting the injection (18)

$$t = 0, \quad r_n < r < \infty, \quad p = p_0 \quad (18)$$

- current pressure gradient state at the needle exit (19)

$$t \geq 0, \quad r = r_n, \quad \frac{\partial p}{\partial r} = - \frac{\eta}{4\pi r_n^2 \varepsilon_0 \chi} G_{vmean} \quad (19)$$

- current pressure state in the tissue far away from injection location (20)

$$t \geq 0, \quad r \rightarrow \infty, \quad p = p_0 \quad (20)$$

According to Crank [7], the problem (16) - (20) analytical solution is given by relation (21) where  $erf(x)$  expresses the error function of argument  $x$ .

$$p(t, r) - p_0 = \frac{G_{vmed} \eta}{4\pi \chi r} \left( 1 - erf\left(\frac{r}{\sqrt{4Dt}}\right) \right) \quad (21)$$

It is observable that at  $r = 0$  the Crank solution has an uncertainty of the type  $\infty * 0$  so it is better to consider instead of condition (19) an equivalent condition, which says that at  $r = r_n$  the pressure is distributed in a sphere of radius  $r_n$  (22)

$$t \geq 0, \quad r = r_n, \quad p(t, r_n) = \frac{1}{V_{rn}} \int_{V_{rn}} p(t, r) dV, \quad V_{rn} = \frac{4}{3} \pi r_n^3 \quad (22)$$

With this univocity condition, the analytical solution pressure diffusion in the tissue reaches the analytical form (23) where the function  $H(r, t)$  is expressed by relation (24)



$$p(t, r) - p_0 = \frac{G_{vmed} \eta}{4\pi\chi V_{rn}} H(r, t) \quad (23)$$

$$H(r, t) = -4r_n(\pi Dt)^{0.5} \exp\left(-\frac{r_n^2}{4Dt}\right) + 4\pi Dt \operatorname{erf}\left(\frac{r}{\sqrt{4Dt}}\right) + 2\pi r_n^2 \left(1 - \operatorname{erf}\left(\frac{r}{\sqrt{4Dt}}\right)\right) \quad (24)$$

Also, with reference to above mentioned singularity elimination, it can be accepted that the pressure at the injection point is equal to the total counterpressure in the tissue, so that the relation (21) can be used in the form (25).

$$\Delta p(t, r) = p(t, r) - p_0 = (p_0 + CP(t)) \left(1 - \operatorname{erf}\left(\frac{r}{\sqrt{4Dt}}\right)\right) \quad (25)$$

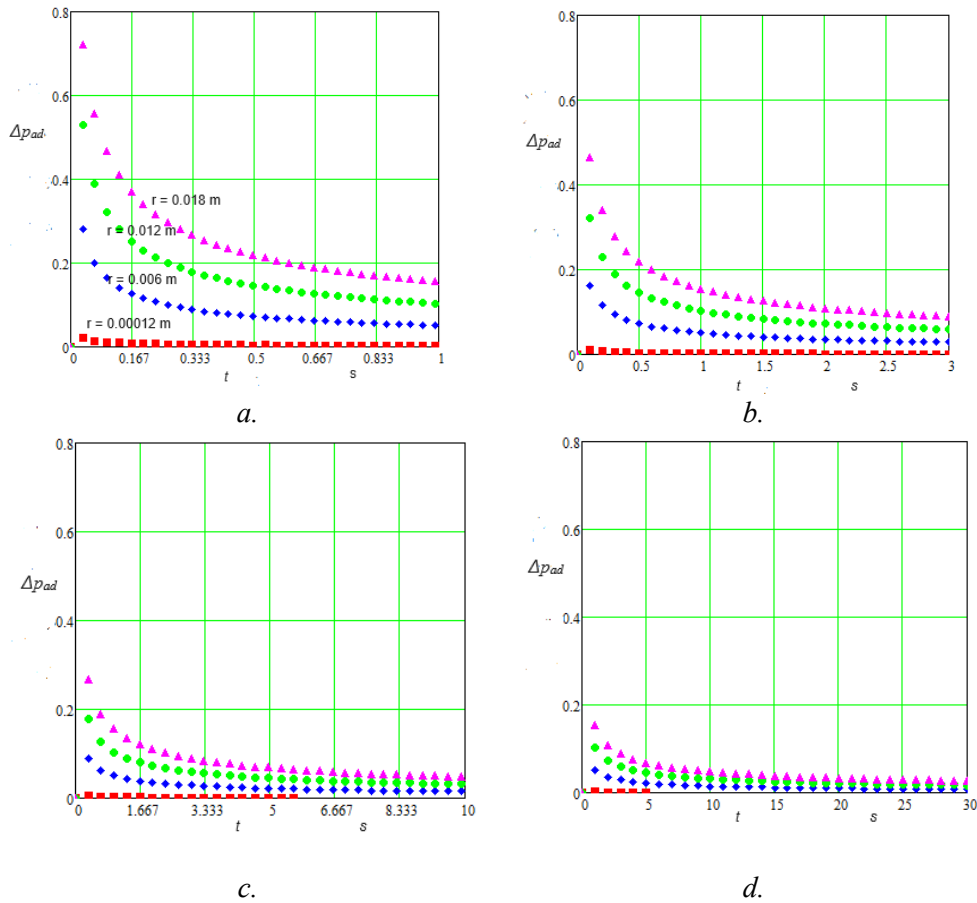


Fig. 7. Time (a-1 s, b - 3 s, c-10 s, d - 30 s) and space (red = 0.00012 m, blue – 0.006 m, green – 0.012 m, magenta 0.018 m from injection point) approach to equilibrium of dimensionless pressure when injecting an insulin solution into the tissue

$$(\chi = 10^{-10} m^2; \alpha = 10^5 Pa, \eta = 10^{-3} kg/(ms)).$$

It is obvious that relation (25) makes it relatively easy to simulate the pressure diffusion in subcutaneous injection of the drug solution.

Figure 7 shows a representation of this pressure distribution for the case syringe needle system injecting of an insulin solution in a tissue from the belly area. Here,  $\Delta p_{ad}$  represents the dimensionless pressure approaching to the state before the injection., defined as relation (26) shows.

$$\Delta p_{ad}(r, t) = 1 - \frac{p(t, r) - p_0}{(p_0 + CP(t))} \quad (26)$$

From figure 7 it is worth noting the rapid pressure diffusion preponderant in a sphere having around 0.006 m. From 0.0006 m to 0.018 m, the diffusion effect is slow. This means that the injected patient feels the injection site as a circle with a diameter over 6 mm, for a time duration less than 30 seconds (figure 7 d)

#### 4. Active drug species diffusion from relaxed deposit to receptors

According with what was presented in the first two paragraphs, we find that the drug species ended up being, following the process of injection and pressure diffusion, located in the liquid in the subcutaneous tissue which has the shape of a sphere with a radius of the order of millimeters (slightly over 6 mm in the example from figure 7). Therefore, whatever the primary drug species is, it ends up, at the completion moment of injection, being cantoned in this deposit, more or less spherical, at a constant concentration level in the interstitial fluid. From this deposit, the drug species will reach the bloodstream, where it is consumed. There is a very large number of models proposed to describe the consumption of the drug species [10]. Regarding the mechanism by which the drug species reaches the consumption circuit (the blood-lymphatic circuit), there are at least two models [11,12]: i) the drug species leaves the initial sphere by diffusion accompanied by a first-order chemical reaction, caused by its transfer in microcapillaries with blood or lymphatic circulation, uniformly distributed in the diffusion field; ii) the drug species diffuses from initial sphere to its border where it is transferred to the consumption system, considered to be concentrated here.

According to the first mechanism, the model describing the transport of drug species to receptors is represented by equation (27) to which the univocity conditions are attached, as it is shown by relations (28)-(30). Here  $c$  is the current drug species concentration in position  $r$  at time  $t$ ,  $D$  is the effective diffusion coefficient of drug species in fibrous tissue in the area where the diffusion of the injection pressure ended and  $k_r$  is an apparent kinetic coefficient, which characterizes the consumption of the drug species through its passage in the consumption circuit

$$\frac{\partial c}{\partial t} = D \frac{1}{r^2} \frac{\partial}{\partial r} \left( r^2 \frac{\partial c}{\partial r} \right) \quad (27)$$

$$t = 0, \quad 0 < r < R_d, \quad c = c_0, \quad R_d \leq r < \infty, \quad c = 0 \quad (28)$$

$$t > 0, r = 0, \frac{dc}{dr} = 0 \quad (29)$$

$$t > 0, r \rightarrow \infty, c = 0 \quad (30)$$

The second mechanism, which considers the initial existence of the drug species inside of system at the limit having the volume established by injection, is that of diffusion in a finite volume with type III boundary conditions at the border. It contains equation (31) and the univocity conditions expressed by relations (32)-(34). As in the case of first model by  $R_d$  it defines the sphere diameter from which the drug diffuses. With  $k_t$  is noted the mass transfer coefficient to sanguine-lymphatic system.

$$\frac{\partial c}{\partial t} = D \frac{1}{r^2} \frac{\partial}{\partial r} \left( r^2 \frac{\partial c}{\partial r} \right) \quad (31)$$

$$t = 0, 0 < r < R_d, c = c_0 \quad (32)$$

$$t > 0, r = 0, \frac{dc}{dr} = 0 \quad (33)$$

$$t > 0, r = R_d, -D \frac{dc}{dr} = k_t c \quad (34)$$

As the first model, the second model, which will be used below to simulate the dynamics of the concentration field of drug species in its cantonment area, has an analytical solution. It is obtained by customizing the method of variables separation [7] to the case described by the set of relations (31) - (34). This solution is expressed by relation (35), in which the problem eigenvalues  $\mu_n$  are solutions of the transcendental equation (36) and the  $A_n$  values are calculable as it is shown by relation (37).

$$c(r, t) = c_0 \sum_{n=1}^{n=\infty} A_n \exp \left( -\mu_n^2 \frac{Dt}{R_d^2} \right) \frac{R_d}{r} \sin \left( \mu_n \frac{r}{R_d} \right) \quad (35)$$

$$\tan(\mu_n) = \frac{\mu_n}{\left( 1 + \frac{k_t R_d}{D} \right)} \quad (36)$$

$$A_n = \frac{\frac{\sin(\mu_n)}{\mu_n^2} - \frac{\cos(\mu_n)}{\mu_n}}{\frac{1}{2} - \frac{\sin(\mu_n) \cos(\mu_n)}{2\mu_n}} \quad (37)$$

If  $R_d$  is estimable between 5 and 10 mm, depending on the patient, as shown in the previous paragraph, for diffusion coefficient inside of  $R_d$  sphere and for frontier

transfer coefficient of drug species values are needed. So, that they cover the specificity for the patient and make the model computed values of drug concentration field in accordance with the experimental observation. Figure 8 shows such dynamics of the concentration field with selected parameters ( $D$  respectively  $k_t$ ), so that the drug species is available in the diffusion volume of the order of days, as shown by most experimental measurements [11,13,14]. The drawing of figure 8 graph was done taking in the summation from the relation (35) only four terms. For the selection made for  $D$ ,  $k_t$  and  $R_d$ , the eigenvalues  $\mu_n$  and coefficients  $A_n$  from table 4 were obtained.

Table 4. Eigenvalues  $\mu_n$  and corresponding  $A_n$  for  $D=10^{-6}$  m<sup>2</sup>/h,  $k_t=4 \cdot 10^{-4}$  m/h,  $R_d=0.008$  m

n	1	2	3	4
$\mu_n$	3.888	7.334	10.619	13.819
$A_n$	0.482	-0.131	0.062	-0.041

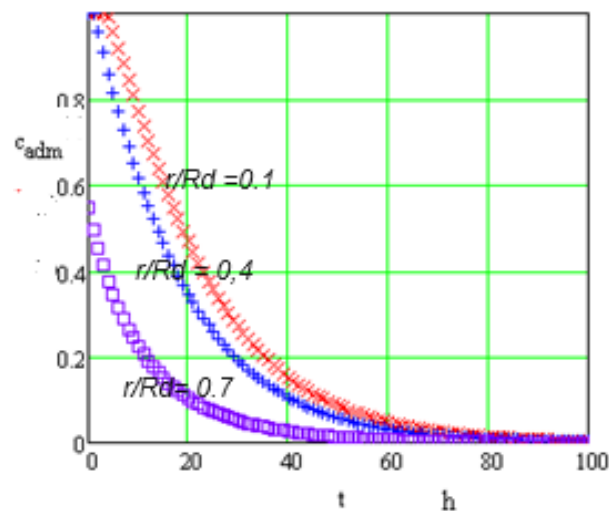


Fig. 8. Dynamics of the dimensionless concentration for three radial positions in the tissue ( $\mu_n$  and  $A_n$  values according to table 4).

From figure 8 it is worth noting that unlike the diffusion process that expresses the spread of pressure field from the injection area, the diffusion of the drug species with its transfer in the lymphatic-blood circuit is a much slower process. A closer look in figure 8 shows that in 20 hours the drug concentration in the location decreases, close to its limit ( $r/R_d = 0.7$ ) below 10% of the initial value. The diffusion model with CL3 at frontier, (31) – (34), has a high sensitivity to their three factors,  $D$ ,  $k_t$  and respectively  $R_d$ .

## 5. Conclusions

The process of injecting of a drug solution into subcutaneous tissue was analyzed, based on fundamental processes that characterize it: a) the hydrodynamics of the flow in the syringe-needle-tissue system, b) the pressure dispersion dynamics in the subcutaneous injection area and, respectively, c) diffusion of drug species from the injection area to the consumption circuit (lymphatic-blood circuit). Respect to hydrodynamic problem of the syringe-needle-tissue system flow, the developed model highlighted the importance of the process factors, especially the response of the tissue to the injection expressed by the injection counterpressure, which is specific to the patient. The simulation of this hydrodynamics for a selected policy for force application on the injection piston is given for the case of injecting an insulin solution with a syringe specific to this case. For dynamics of pressure dispersion in the injection area, a diffusion type model was obtained, and this pressure dispersion was simulated for injection of an insulin solution. Was find that pressure dispersion occurs under 30 seconds, manifesting itself in a sphere with a radius around of 12 mm. In this case, the properties of the tissue are expressed by its permeability to flow and by the fraction of liquid in it. For the diffusion of drug species from injection area to the consumption circuit, a finite volume diffusion model with type III boundary conditions at frontier was chosen. The selected simulation case was highlighted that this process is a slow one, the drug species still existing in the injection area even after 20-30 hours.

## References

- [1] Kermode M., *Unsafe Injections in Low-income Country Health Settings: Need for Injection Safety Promotion to Prevent the Spread of Blood-borne Viruses*, Health Promot. Int., **19**, 2004, p. 95- 103.
- [2] Nir Y., Paz A., Sabo E., Potsman I., *Fear of Injection in Young Adults: Prevalence and Associations*, Am. J. Trop. Med. Hyg., **68**, 2003, p. 341- 344.
- [3] Mitragotri S., *Immunization without Needles*, Nature Rev. Immunol., **5**, 2005, p. 905-916.
- [4] Yoshiyuki T., Oudolov N., Ghalbzouri A.El., Chao S., Loshe D., *Needle – free Injection into Skin and Soft Matter with Highly Focused Microjets*, arXIV:1201. 1907v2 [physics.flu-dyn] 15 oct 2012.
- [5] Dobre T., Floarea O., *Momentum Transfer*, Ed. Matrix Rom, Bucharest, 1997.
- [6] Thomsen Maria, *Subcutaneous Injections: Visualization and Optimizing Device- tissue Interaction*, PhD Thesis, University of Copenhagen, 2015.
- [7] Crank J., *Mathematics of Diffusion*, Clarendon Press, Oxford, 2<sup>th</sup> Edition, 1975.
- [8] Radboud M. N., *Fluid Mechanics in Intratechal Drug Delivery*, PhD Thesis, Ecole Polytechnique Federale de Laussane, 2008.
- [9] Duran-Reynals F., *Studies on the Localization of Dyes and Foreign Proteins in Normal and Malignant Tissues*, Am. J. Cancer, **35**, 1939, p. 98-107.
- [10] David W.A. B., *Mathematical Modeling of Pharmacokinetic Data*, Taylor & Francis, CRC Press, 1995.
- [11] Tornoe W. Ch., Agerso H., Nielsen A. H., Madsen H., Jonsson N. E., *Population Pharmacokinetic Modeling of a Subcutaneous Depot for GmRH Antagonist Degarelix*, Pharmaceutical Research, **21**, 4, 2004, p. 574-584.
- [12] Zhou H., *Pharmacokinetic Strategies in Deciphering Atypical Drug Absorption Profiles*, J. Clin. Pharmacol., **43**, 2003, p. 211-227.
- [13] Aristides D., Panos M., *Fractional Kinetics in Drug Absorption and Disposition Processes*, Journal of Pharmacokinetics and Pharmacodynamics, **36**, 2009, p. 165–178.

- [14] Rocchetti M., Simeoni M., Pesenti E., Nicolao De G., Poggesi I., *Predicting the Active Doses in Humans from Animal Studies: A Novel Approach in Oncology*. European Journal of Cancer, **43**, 12, 2007, p. 1862 – 1868.